Subtleties in Tolerating Correlated Failures in Wide-area Storage Systems

Suman Nath*
Microsoft Research
sumann@microsoft.com

Haifeng Yu Phillip B. Gibbons
Intel Research Pittsburgh
{*haifeng.yu,phillip.b.gibbons*}*@intel.com*

Srinivasan Seshan
Carnegie Mellon University
srini@cmu.edu

Abstract

High availability is widely accepted as an explicit requirement for distributed storage systems. Tolerating correlated failures is a key issue in achieving high availability in today's wide-area environments. This paper systematically revisits previously proposed techniques for addressing correlated failures. Using several real-world failure traces, we qualitatively answer four important questions regarding how to design systems to tolerate such failures. Based on our results, we identify a set of design principles that system builders can use to tolerate correlated failures. We show how these lessons can be effectively used by incorporating them into IRISSTORE, a distributed read-write storage layer that provides high availability. Our results using IRISSTORE on the PlanetLab over an 8-month period demonstrate its ability to withstand large correlated failures and meet preconfigured availability targets.

1 Introduction

High availability is widely accepted as an explicit requirement for distributed storage systems (e.g., [8, 9, 10, 14, 15, 19, 23, 42]). This is partly because these systems are often used to store important data, and partly because performance is no longer the primary limiting factor in the utility of distributed storage systems. Under the assumption of failure independence, replicating or erasure coding the data provides an effective way to mask individual node failures. In fact, most distributed storage systems today use some form of replication or erasure coding.

In reality, the assumption of failure independence is rarely true. Node failures are often correlated, with multiple nodes in the system failing (nearly) simultaneously. The size of these correlated failures can be quite large. For example, Akamai experienced large distributed denial-of-service (DDoS) attacks on its servers in May and June 2004 that resulted in the unavailability of many of its client sites [1]. The PlanetLab experienced four failure events during the first half of 2004 in which more than 35 nodes ($\approx 20\%$) failed within a few minutes. Such large correlated failure events may have numerous causes, including system software bugs, DDoS attacks, virus/worm infections, node overload, and human errors. The impact of failure correlation on system unavailability is dramatic (i.e., by orders of magnitude) [6, 38]. As a result, tolerating correlated failures is a key issue in designing highly-available distributed storage systems. Even though researchers have long been aware of correlated failures, most systems [8, 9, 10, 14, 15, 41, 42] are still evaluated and compared under the assumption of independent failures.

In the context of the IrisNet project [17], we aim to design and implement a distributed read/write storage layer that provides high availability despite correlated node failures in non-P2P wide-area environments (such as the PlanetLab and Akamai). We study three real-world failure traces for such environments to evaluate the impact of realistic failure patterns on system designs. We frame our study around providing quantitative answers to several important questions, some of which involve the effectiveness of existing approaches [19, 37]. We show that some existing approaches, although plausible, are less effective than one might hope under real-world failure correlation, often resulting in system designs that are far from optimal. Our study also reveals the subtleties that cause this discrepancy between the expected behavior and the reality. These new findings lead to four design principles for tolerating correlated failures. While some of the findings are perhaps less surprising than others, none of the findings and design principles were explicitly identified or carefully quantified prior to our work. These design principles are applied and implemented in our highly-available read/write storage layer called IRISSTORE.

Our study answers the following four questions about tolerating correlated failures:

Can correlated failures be avoided by history-based failure pattern prediction? We find that avoiding correlated failures by predicting the failure pattern based on externally-observed failure history (as proposed in OceanStore [37]) provides *negligible* benefits in alleviating the negative effects of correlated failures in our real-world

*Work done while this author was a graduate student at CMU and an intern at Intel Research Pittsburgh.

failure traces. The subtle reason is that the top 1% of correlated failures (in terms of size) have a dominant effect on system availability, and their failure patterns seem to be the most difficult to predict.

Is simple modeling of failure sizes adequate? We find that considering only a single (maximum) failure size (as in Glacier [19]) leads to suboptimal system designs. Under the same level of failure correlation, the system configuration as obtained in [19] can be both overly-pessimistic for lower availability targets (thereby wasting resources) and overly-optimistic for higher availability targets (thereby missing the targets). While it is obvious that simplifying assumptions (such as assuming a single failure size) will always introduce inaccuracy, our contribution is to show that the inaccuracy can be dramatic in practical settings. For example, in our traces, assuming a single failure size leads to designs that either waste 2.4 times the needed resources or miss the availability target by 2 nines. Hence, more careful modeling is crucial. We propose using a bi-exponential model to capture the distribution of failure sizes, and show how this helps avoid overly-optimistic or overly-pessimistic designs.

Are additional fragments/replicas always effective in improving availability? For popular $(n/2)$-out-of-n encoding schemes (used in OceanStore [23] and CFS [10]), as well as majority voting schemes [35] over n replicas, it is well known that increasing n yields an exponential decrease in unavailability under independent failures. In contrast, we find that under real-world failure traces with correlated failures, additional fragments/replicas result in a strongly diminishing return in availability improvement for many schemes including the previous two. It is important to note that this diminishing return does *not* directly result from the simple presence of correlated failures. For example, we observe no diminishing return under Glacier's single-failure-size correlation model. Rather, in our real-world failure traces, the diminishing return arises due to the combined impact of correlated failures of different sizes. We further observe that the diminishing return effects are so strong that even doubling or tripling n provides only limited benefits after a certain point.

Do superior designs under independent failures remain superior under correlated failures? We find that the effects of failure correlation on different designs are dramatically different. Thus selecting between two designs $\mathcal{D}$ and $\mathcal{D}'$ based on their availability under independent failures may lead to the wrong choice: $\mathcal{D}$ can be far superior under independent failures but far inferior under real-world correlated failures. For example, our results show that while 8-out-of-16 encoding achieves 1.5 more nines of availability than 1-out-of-4 encoding under independent failures, it achieves 2 fewer nines than 1-out-of-4 encoding under correlated failures. Thus, system designs must be explicitly evaluated under correlated failures.

Our findings, unavoidably, depend on the failure traces we used. Among the four findings, the first one may be the most dependent on the specific traces. The other three findings, on the other hand, are likely to hold as long as failure correlation is non-trivial and has a wide range of failure sizes.

We have incorporated these lessons and design principles into our IRISSTORE prototype: IRISSTORE does not try to avoid correlated failures by predicting the correlation pattern; it uses a failure size distribution model rather than a single failure size; and it explicitly quantifies and compares configurations via online simulation with our correlation model. As an example application, we built a publicly-available distributed wide-area network monitoring system on top of IRISSTORE, and deployed it on over 450 PlanetLab nodes for 8 months. We summarize our performance and availability experience with IRISSTORE, reporting its behavior during a highly unstable period of the PlanetLab (right before the SOSP 2005 conference deadline), and demonstrating its ability to reach a pre-configured availability target.

2 Background and Related Work

Distributed storage systems and erasure coding. Distributed storage systems [8, 9, 10, 14, 15, 19, 23, 42] have long been an active area in systems research. Of these systems, only OceanStore [23] and Glacier [19] explicitly consider correlated failures. OceanStore uses a distributed hash table (DHT) based design to support a significantly larger user population (e.g., 10^{10} users) than previous systems. Glacier is a more robust version of the PAST [32] DHT-based storage system that is explicitly designed to tolerate correlated failures.

Distributed storage systems commonly use data redundancy (replication, erasure coding [31]) to provide high availability. In erasure coding, a data object is encoded into n *fragments*, out of which any m fragments can reconstruct the object. OceanStore uses $(n/2)$-out-of-n erasure coding. This configuration of erasure coding is also used by the most recent version of CFS [10, 13], one of the first DHT-based, read-only storage systems. Glacier, on the other hand, *adapts* the settings of m and n to achieve availability and resource targets. Replication can be viewed as a special case of erasure coding where $m = 1$.

In large-scale systems, it is often desirable to automatically create new fragments upon the loss of existing ones (due to node failures). We call such systems *regeneration* systems. Almost all recent distributed storage systems (including OceanStore, CFS, and our IRISSTORE system) are regeneration systems. Under the assumption of failure independence, the availability of regeneration systems is typically analyzed [42] using a Markov chain to model the birth-death process.

Trace	Duration	Nature of nodes	# of nodes	Probe interval	Probe method
PL_trace [3]	03/2003 to 06/2004	PlanetLab nodes	277 on avg	15 to 20 mins	all-pair pings; 10 ping packets per probe
WS_trace [6]	09/2001 to 12/2001	Public web servers	130	10 mins	HTTP GET from a CMU machine
RON_trace [4]	03/2003 to 10/2004	RON testbed	30 on avg	1 to 2 mins	all-pair pings; 1 ping packet per probe

Table 1: *Three traces used in our study.*

Previous availability studies of correlated failures. Traditionally, researchers assume failure independence when studying availability [8, 9, 10, 14, 15, 41, 42]. For storage systems, correlated failures have recently drawn more attention in the context of wide-area environments [11, 19, 22, 37, 38], local-area and campus network environments [9, 34], and disk failures [6, 12]. None of these previous studies point out the findings and design principles in this paper or quantify their effects. Below, we focus on those works most relevant to our study that were not discussed in the previous section.

The Phoenix Recovery Service [22] proposes placing replicas on nodes running heterogeneous versions of software, to better guard against correlated failures. Because their target environment is a heterogeneous environment such as a peer-to-peer system, their approach does not conflict with our findings.

The effects of correlated failures on erasure coding systems have also been studied [6] in the context of survivable storage disks. The study is based on availability traces of desktops [9] and different Web servers. (We use the same Web server trace in our study.) However, because the target context in [6] is disk drives, the study considers much smaller-scale systems (at most 10 disks) than we do.

Finally, this paper establishes a bi-exponential model to fit correlated failure size distribution. Related to our work, Nurmi et al. [30] show that machine availability (instead of failure sizes) in enterprise and wide-area distributed systems also follows hyper-exponential (a more general version of our bi-exponential model) models.

Data maintenance costs. In addition to availability, failure correlation also impacts data maintenance costs (i.e., different amounts of data transferred over the network in regenerating the objects). Weatherspoon et al. [36] show that the maintenance costs of random replica placement (with small optimizations) are similar to those of an idealized optimal placement where failure correlation is completely avoided. These results do not conflict with our conclusion that random replica placement (or even more sophisticated placement) cannot effectively alleviate the negative effects of failure correlation on availability.

3 Methodology

This study is based on system implementation and experimental evaluation. The experiments use a combination of three testbeds: live PlanetLab deployment, real-time emulation on Emulab [2], and event-driven simulation. Each testbed allows progressively more extensive evaluation than the previous one. Moreover, the results from one testbed help validate the results from the next testbed.

In this paper, we use ERASURE(m, n) to denote an m-out-of-n read-only erasure coding system. Also, to unify terminology, we often refer to replicas as fragments of an ERASURE$(1, n)$ system. Unless otherwise mentioned, all designs we discuss in this paper use regeneration to compensate for lost fragments due to node failures.

For the purpose of studying correlated failures, a *failure event* (or simply *failure*) crashes one or more nodes in the system. The number of nodes that crash is called the *size* of the failure. To distinguish a failure event from the failures of individual nodes, we explicitly call the latter *node failures*. A data object is *unavailable* if it can not be reconstructed due to failures. We present availability results using standard "number of nines" terminology (i.e., $\log_{0.1}(\phi)$, where ϕ is the probability that the data object is unavailable).

Failure traces. We use three real-world wide-area failure traces (Table 1) in our study. WS_trace is intended to be representative of public-access machines that are maintained by different administrative domains, while PL_trace and RON_trace potentially describe the behavior of a centrally administered distributed system that is used mainly for research purposes, as well as for a few long running services.

A probe *interval* is a complete round of all pair-pings or Web server probes. PL_trace and RON_trace consist of periodic probes between every pair of nodes. Each probe may consist of multiple pings; we declare that a node has *failed* if *none* of the other nodes can ping it during that interval. We do not distinguish between whether the node has failed or has simply been partitioned from all other nodes—in either case it is unavailable to the overall system. WS_trace contains logs of HTTP GET requests from a single node at CMU to multiple Web servers. Our evaluation of this trace is not as precise because near-source network partitions make it appear as if all the other nodes have failed. To mitigate this effect, we assume that the probing node is disconnected from the network if 4 or more consecutive HTTP requests to different servers fail.[1] We then ignore all failures during that probe period. This heuristic

[1] This threshold is the smallest to provide a plausible number of near-source partitions. Using a smaller threshold would imply that the client (on Internet2) experiences a near-source partition $> 4\%$ of the time in our trace, which is rather unlikely.

# nodes affected by the gap	number of such gaps
all	7
7	1
6	3
4	1
3	6
2	22
1	123

Table 2: *We group gaps by the number of nodes affected, and then count the number of gaps in each category.*

may still not perfectly classify source and server failures, but we believe that the error is likely to be minimal.

In PL_trace, many periods of time appear in the trace where probe information is not available for all nodes. We call each such period of time as a *gap*. For those nodes that do not have probe information in a given gap, we say they are *affected* by the gap. These gaps occur in the trace primarily due to two reasons – (1) the affected node was removed from the production list of PlanetLab and added back later to the list, because of some problem with the node; (2) the central server that collects all-pair-ping measurements failed. In our study, we consider gaps due to the first reason as the failures of the affected nodes, since these nodes were removed from the infrastructure and not available for use. For gaps due to the second reason, we assume that the status (i.e, up or down) of the affected nodes do not change during those gaps. To determine which gap is due to which reason, we classify the gaps in the trace by the number of affected nodes in the gaps (Table 2). All together we find 163 gaps in the trace. Seven gaps affect all nodes (over 300 nodes). This is a clear evidence of central server failure. On the other hand, all other gaps affect 7 or fewer nodes, which are indications of node removals. Not having gaps affecting more than 7 but less than 300 nodes confirms that the gaps are most likely caused by the previous two reasons (which result in quite different gap behavior).

In studying correlated failures, each probe interval is considered as a separate failure event whose size is the number of failed nodes that were available during the previous interval. In PL_trace, the set of nodes in each interval are constantly changing due to node join and leave. The same is true in WS_trace because of the previous filtering step we use, which filters some of the nodes in certain intervals. The change in WS_trace, however, is rather small. In these two traces, when counting the number of failed nodes that were not failed as of the previous interval (to determine the size of the failure event), the nodes counted must be present in both intervals, so that we can say it transits from "up" to "down". Similarly, when calculating MTTF, we must first observe one transition from "down" to "up" (where the node must be present in two adjacent intervals), and then observe a transition from "up" to "down" (similarly, the node must be present in two adjacent intervals). Further, the node must always be in the trace between the two transitions. Only in such a scenario will the time between the two transitions contribute to our calculation of MTTF. The same is true when we calculate MTTR. This is the same methodology as in previous studies [11] of these traces. Finally, due to the limited duration of the traces, and also because failures (especially large correlated failures) are rare events, we do not observe occurrences of all failure sizes. On the other hand, we cannot simply use a probability of zero for those failure sizes, since zero would be negative infinity on log-scale. We thus use the following smoothing technique. Consider a sequence of consecutive failure sizes x, $x+1$, ..., $x+k-1$ for which we do not observe any events, but we do observe z failure events with size of $x+k$. Then we treat the z events as z/k failure events for each of the failure sizes of x, $x+1$, ..., $x+k-1$, $x+k$. Notice that such processing will only underestimate the strength of correlation, since it treats some of the larger failures as smaller failures. Also, the processing has larger impact on WS_trace than on PL_trace and RON_trace.

Limitations. Although the findings from this paper depend on the traces we use, the effects observed in this study are likely to hold as long as failure correlation is non-trivial and has a wide range of failure sizes. One possible exception is our observation about the difficulty in predicting failure patterns of larger failures. However, we believe that the sources of some large failures (e.g., DDoS attacks) make accurate prediction difficult in any deployment.

Because we target IRISSTORE's design for non-P2P environments, we intentionally study failure traces from systems with largely homogeneous software (operating systems, etc.). Even in WS_trace, over 78% of the web servers were using the same Apache server running over Unix, according to the historical data at http://www.netcraft.com. We believe that wide-area non-P2P systems (such as Akamai) will largely be homogeneous because of the prohibitive overhead of maintaining multiple versions of software. Failure correlation in P2P systems can be dramatically different from other wide-area systems, because many failures in P2P systems are caused by user departures. In the future, we plan to extend our study to P2P environments. Another limitation of our traces is that the long probe intervals prevent the detection of short-lived failures. This makes our availability results slightly optimistic.

Steps in our study. Section 4 constructs a tunable failure correlation model from our three failure traces; this model allows us to study the sensitivity of our findings beyond the three traces. Sections 5–8 present the questions we study, and their corresponding answers, overlooked sub-

tleties, and design principles. These sections focus on read-only ERASURE(m, n) systems, and mainly use trace-driven simulation, supplemented by model-driven simulation for sensitivity study. Section 9 shows that our conclusions readily extend to read/write systems. Section 10 describes and evaluates IRISSTORE, including its availability running on PlanetLab for an 8-month period. Finally, in Section 11, our IRISSTORE deployment on PlanetLab is used to validate the accuracy of our simulation.

4 A Tunable Model for Correlated Failures

This section constructs a tunable failure correlation model from the three failure traces. The primary purpose of this model is to allow sensitivity studies and experiments with correlation levels that are stronger or weaker than in the traces. In addition, the model later enables us to avoid overly-pessimistic and overly-optimistic designs. The model balances idealized assumptions (e.g., Poisson arrival of correlated failures) with realistic characteristics (e.g., mean-time-to-failure and failure size distribution) extracted from the real-world traces. In particular, it aims to accurately capture large (but rare) correlated failures, which have a dominant effect on system unavailability.

4.1 Correlated Failures in Real Traces

We start by investigating the failure correlation in our three traces. Figure 1 plots the PDF of failure event sizes for the three traces. Because of the finite length of the traces, we cannot observe events with probability less than 10^{-5} or 10^{-6}. While `RON_trace` and `WS_trace` have a roughly constant node count over their entire duration, there is a large variation in the total number of nodes in `PL_trace`. To compensate, we use both raw and normalized failure event sizes for `PL_trace`. The normalized size is the (raw) size multiplied by a normalization factor γ, where γ is the average number of nodes (i.e., 277) in `PL_trace` divided by the number of nodes in the interval.

In all traces, Figure 1 shows that failure correlation has different strengths in two regions. In `PL_trace`, for example, the transition between the two regions occurs around event size 10. In both regions, the probability decreases roughly exponentially with the event size (note the log-scale of the y-axis). However, the probability decreases significantly faster for small-scale correlated failures than for large-scale ones. We call such a distribution *bi-exponential*. Although we have only anecdotal evidence, we conjecture that different failure causes are responsible for the different parts of the distribution. For example, we believe that system instability, some application bugs, and localized network partitions are responsible for the small failure events. It is imaginable that the probability decreases quickly as the scale of the failure increases. On the other hand, human interference, attacks, viruses/worms and large ISP failures are likely to be responsible for the large failures. This is supported by the fact that many of the larger PlanetLab failures can be attributed to DDoS attacks (e.g., on 12/17/03), system software bugs (e.g., on 3/17/04), and node overloads (e.g., on 5/14/04). Once such a problem reaches a certain scale, extending its scope is not much harder. Thus, the probability decreases relatively slowly as the scale of the failure increases.

4.2 A Tunable Bi-Exponential Model

In our basic failure model, failure events arrive at the system according to a Poisson distribution. The entire system has a *universe* of u nodes. The model does not explicitly specify which of the u nodes each failure event crashes, for the following reasons: Predicting failure patterns is not an effective means for improving availability, and pattern-aware fragment placement achieves almost identical availability as a pattern-oblivious random placement (see Section 5). Thus, our availability study needs to consider only the case where the m fragments of a data object are placed on a random set of m nodes. Such a random placement, in turn, is equivalent to using a fixed set of m nodes and having each failure event (with size s) crash a random set of s nodes in the universe. Realizing the above point helps us to avoid the unnecessary complexity of modeling which nodes each failure event crashes – each failure event simply crashes a random set of s nodes.

We find that many existing distributions (such as heavy-tail distributions [25]) cannot capture the bi-exponential property in the trace. Instead, we use a model that has two exponential components, one for each region. Each component has a tunable parameter ρ between 0 and ∞ that intuitively captures the slope of the curve and controls how strong the correlations are. When $\rho = 0$, failures are independent, while $\rho = \infty$ means that every failure event causes the failure of all u nodes. Specifically, for $0 < \rho < \infty$, we define the following geometric sequence: $f(\rho, i) = c(\rho) \cdot \rho^i$. The normalizing factor $c(\rho)$ serves to make $\sum_{i=0}^{u} f(\rho, i) = 1$.

We can now easily capture the bi-exponential property by composing two $f(\rho, i)$. Let p_i be the probability of failure events of size i, for $0 \leq i \leq u$. Our correlation model, denoted as $G(\alpha, \rho_1, \rho_2)$, defines $p_i = (1 - \alpha) f(\rho_1, i) + \alpha f(\rho_2, i)$, where α is a tunable parameter that describes the probability of large-scale correlated failures. Compared to a piece-wise function with different ρ's for the two regions, $G(\alpha, \rho_1, \rho_2)$ avoids a sharp turning point at the boundary between the two regions.

Figure 1 shows how well this model fits the three traces. The parameters of the models are chosen such that the Root Mean Square errors between the models and the trace points are minimized. Because of space limitations, we are

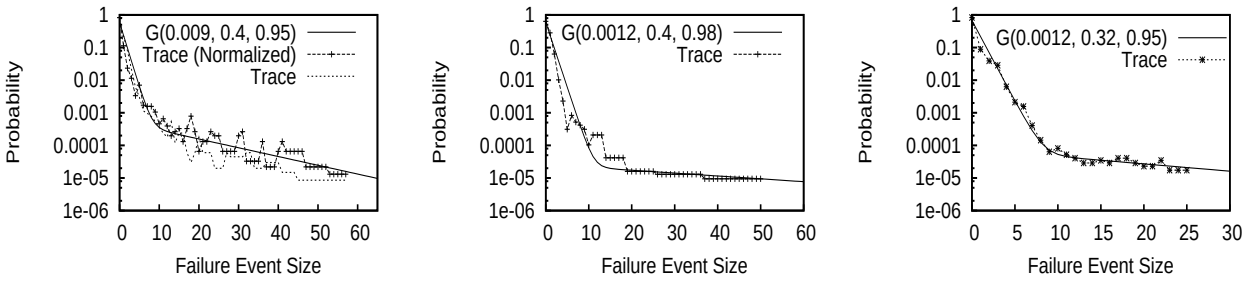

(a) PL_trace (b) WS_trace (c) RON_trace

Figure 1: *Correlated failures in three real-world traces. $G(\alpha, \rho_1, \rho_2)$ is our correlation model.*

only able to provide a brief comparison among the traces here. The parameters of the model are different across the traces, in large part because the traces have different universe sizes (10 node failures out of 277 nodes is quite different from 10 node failures out of 30 nodes). As an example of a more fair comparison, we selected 130 random nodes from PL_trace to enable a comparison with WS_trace, which has 130 nodes. The resulting trace is well-modeled by $G(0.009, 0.3, 0.96)$. This means that the probability of large-scale correlated failures in PL_trace is about 8 times larger than WS_trace.

Failure arrival rate and recovery. So far the correlation model $G(\alpha, \rho_1, \rho_2)$ only describes the failure event size distribution, but does not specify the event arrival rate. To study the effects of different levels of correlation, the event arrival rate should be such that the average mean-time-to-failure (MTTF) of nodes in the traces is always preserved. Otherwise with a constant failure event arrival rate, increasing the correlation level would have the strong side effect of decreasing node MTTFs. To preserve the MTTF, we determine the system-wide failure event arrival rate λ to be such that $1/(\lambda \sum_{i=1}^{u}(ip_i)) = \text{MTTF}/u$.

We observe from the traces that, in fact, there exists non-trivial correlation among node recoveries as well. Moreover, nodes in the traces have non-uniform MTTR and MTTF. However, our experiments show that the above two factors have little impact on system availability for our study. Specifically, for all parameters we tested (e.g., later in Figure 5), the availability obtained under model-driven simulation (which assumes independent recoveries and uniform MTTF/MTTR) is almost identical to that obtained under trace-driven simulation (which has recovery correlation and non-uniform MTTF/MTTR). Therefore, our model avoids the unnecessary complexity of modeling recovery correlation and non-uniform MTTF/MTTR.

4.3 Stability of the Model

Convergence. We first study the convergence properties of our model, using PL_trace and RON_trace (we do not use WS_trace because of its short duration). For each trace, we obtain a "reference model" using the entire trace. Then, we consider successively longer portions of the trace, and compute its difference from the reference model. For our metric, we use *mean relative difference* (MRD), defined as the average of $|p_{i,t} - p_{i,m}|/p_{i,m}$ for all i's, where $p_{i,t}$ ($p_{i,m}$) is the probability of size-i failures from the trace portion (from the model, respectively). Intuitively, a small MRD means that the trace portion matches the reference model well.

Figure 2(a) plots the MRD between the reference models and suffixes of the traces, as a function of the length of the suffixes. For both traces, the figure shows that the MRD roughly monotonically decreases as we use a longer and longer trace. Also, the curves flatten after roughly 4 or 5 months. This means that the model does converge and the convergence time is roughly several months. We believe this convergence time is quite good given the rarity of large correlation events. For both traces, the MRD after 5 months is below 0.8. Note that the MRD from the model fittings in Figure 1 are 0.64, 0.60, and 0.24 for PL_trace, WS_trace, and RON_trace, respectively. This means that an MRD of 0.8 is quite satisfactory.

Effectiveness over time. Our model will later be used (among other things) to configure IRISSTORE to achieve a given availability target. To be effective for such purposes, the model built ("trained") using a prefix of a trace should reflect well the failures occurring in the rest of the trace. To test this, we build models using the 2003 portions of RON_trace and PL_trace, and then compare these models to the 2004 portions of the respective traces. We find that the MRD is roughly 0.7 and 0.3 for PL_trace and RON_trace, respectively. Figures 2(b) and (c) provide a direct comparison of the availability achieved under the 2003-based models versus under the 2004 traces. In all cases, the availability difference is below half a nine. These results suggest that configuring IRISSTORE using the 2003-based model would have indeed been effective for reaching availability targets in 2004.

In the next four sections, we will address each of the four questions from Section 1. Unless otherwise stated, all our results are obtained via event-driven simulation (including data regeneration) based on the three real failure traces. The bi-exponential model is used only when we

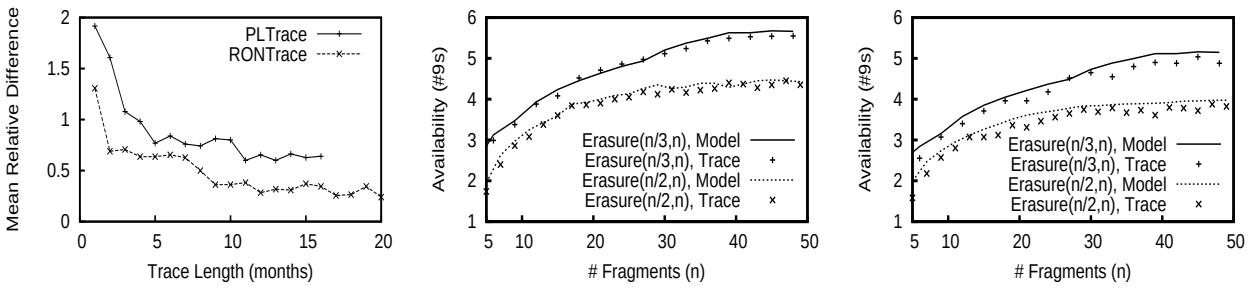

(a) Difference between reference models and traces of different lengths

(b) Predicted and actual availability under `RON_trace`

(c) Predicted and actual availability under `PL_trace`

Figure 2: *Stability of model*

need to tune the correlation level—in such cases we will explicitly mention its use. As mentioned earlier, the accuracy of our simulator has been carefully validated against live deployment results on the PlanetLab and also emulation results on Emulab. Because many existing systems (e.g., OceanStore, Glacier, and CFS) use a large number of fragments, we show results for up to $n = 60$ fragments (as well as for large values of m).

5 Can Correlated Failures be Avoided by History-based Failure Pattern Prediction?

Chun et al. [11] point out that externally observed node failure histories (based on probing) can be used to discover a relatively stable pattern of correlated failures (i.e., which set of nodes tend to fail together), based on a portion of `PL_trace`. Weatherspoon et al. [37] (as part of the OceanStore project [23]) reach a similar conclusion by analyzing a four-week failure trace of 306 web servers[2]. Based on such predictability, they further propose a framework for online monitoring and clustering of nodes. Nodes within the same cluster are highly correlated, while nodes in different clusters are more independent. They show that the clusters constructed from the first two weeks of their trace are similar to those constructed from the last two weeks. Given the stability of the clusters, they conjecture that by placing the n fragments (or replicas) in n different clusters, the n fragments will not observe excessive failure correlation among themselves. In some sense, the problem of correlated failures goes away.

Our Finding. We carefully quantify the effectiveness of this technique using the same method as in [37] to process our failure traces. For each trace, we use the first half of the trace (i.e., "training data") to cluster the nodes using the same clustering algorithm [33] as used in [37]. Then, as a case study, we consider two placement schemes of an ERASURE$(n/2, n)$ (as in OceanStore) system. The first scheme (*pattern-aware*) explicitly places the n fragments of the same object in n different clusters, while the second scheme (*pattern-oblivious*) simply places the fragments on n random nodes. Finally, we measure the availability under the second half of the trace.

We first observe that most ($\approx 99\%$) of the failure events in the second half of the traces affect only a very small number (≤ 3) of the clusters computed from the first half of the trace. This implies that the clustering of correlated nodes is relatively stable over the two halves of the traces, which is consistent with [37].

On the other hand, Figure 3 plots the achieved availability of the two placement schemes under `WS_trace` and `PL_trace`. We do not use `RON_trace` because it contains too few nodes. The graph shows that explicitly choosing different clusters to place the fragments gives us *negligible* improvement on availability. We also plot the availability achieved if the failures in `WS_trace` were independent. This is done via model-driven simulation and by setting the parameters in our bi-exponential model accordingly. Note that under independent failures, the two placement schemes are identical. The large differences between the curve for independent failures and the other curves show that there are strong negative effects from failure correlation in the trace. Identifying and exploiting failure patterns, however, has almost no effect in alleviating such impacts. We have also obtained similar findings under a wide-range of other m and n values for ERASURE(m, n).

A natural question is whether the above findings are because our traces are different from the traces studied in [11, 37]. Our `PL_trace` is, in fact, a superset of the failure trace used in [11]. On the other hand, the failure trace studied in [37], which we call `Private_trace`, is not publicly available. Is it possible that `Private_trace` gives even better failure pattern predictability than our traces, so that pattern-aware placement would indeed be effective? To answer this question, we directly compare the "pattern predictability" of the traces using the metric from [37]: the *average mutual information among the clusters* (MI) (see [37] for a rigorous definition). A smaller MI means that the clusters constructed from the training data predict the fail-

[2]The trace actually contains 1909 web servers, but the authors analyzed only 306 servers because those are the only ones that ever failed during the four weeks.

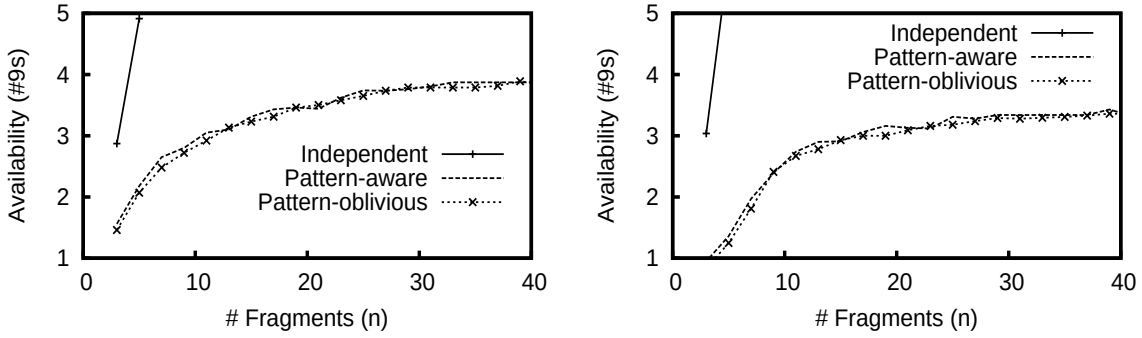

(a) WS_trace (b) PL_trace

Figure 3: *Negligible availability improvements from failure pattern prediction for* ERASURE$(n/2, n)$ *systems.*

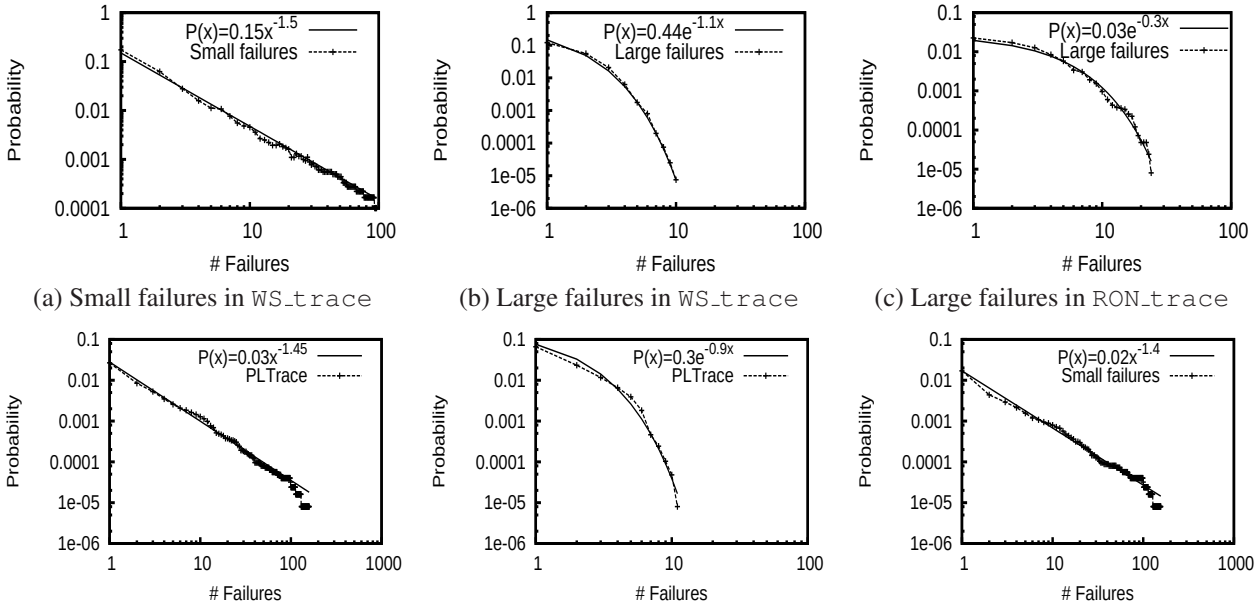

(a) Small failures in WS_trace (b) Large failures in WS_trace (c) Large failures in RON_trace

(d) Small failures in PL_trace (e) Large failures in PL_trace (f) Small failures in RON_trace

Figure 4: *Predictability of pairwise failures. For two nodes selected at random, the plots show the probability that the pair fail together (in correlation) more than x times during the entire trace. Distributions fitting the curves are also shown.*

ure patterns in the rest of the trace better. Weatherspoon et al. report an MI of 0.7928 for their Private_trace. On the other hand, the MI for our WS_trace is 0.7612. This means that the failure patterns in WS_trace are actually more "predictable" than in Private_trace.

The Subtlety. To understand the above seemingly contradictory observations, we take a deeper look at the failure patterns. To illustrate, we classify the failures into small failures and large failures based on whether the failure size exceeds 15. With this classification, in all traces, most ($\approx 99\%$) of the failures are small.

Next, we investigate how accurately we can predict the failure patterns for the two classes of failures. We use the same approach [20] used for showing that UNIX processes running for a long time are more likely to continue to run for a long time. For a random pair of nodes in WS_trace, Figure 4(a) plots the probability that the pair crashes together (in correlation) more than x times because of the small failures. The straight line in log-log scale indicates that the data fits the Pareto distribution of $P(\#failure \geq x) = cx^{-k}$, in this case for $k = 1.5$. We observe similar fits for PL_trace ($P(\#failure \geq x) = 0.3x^{-1.45}$) and RON_trace ($P(\#failure \geq x) = 0.02x^{-1.4}$). Such a fit to the Pareto distribution implies that pairs of nodes that have failed together many times in the past are more likely to fail together in the future [20]. Therefore, past pairwise failure patterns (and hence the clustering) caused by the small failures are likely to hold in the future.

Next, we move on to large failure events (Figure 4(b)). Here, the data fit an exponential distribution of

$P(\#failure \geq x) = ae^{-bx}$. The memoryless property of the exponential distribution means that the frequency of future correlated failures of two nodes is independent of how often they failed together in the past. This in turn means that we cannot easily (at least using existing history-based approaches) predict the failure patterns caused by these large failure events. Intuitively, large failures are generally caused by external events (e.g., DDoS attacks), occurrences of which are not predictable in trivial ways. We observe similar results in the other two traces. For example, Figure 4(c) shows an exponential distribution fit for the large failure events in `RON_trace`. For `PL_trace`, the fit is $P(\#failure \geq x) = 0.3e^{-0.9x}$.

Thus, the pattern for roughly 99% of the failure events (i.e., the small failure events) is predictable, while the pattern for the remaining 1% (i.e., the large failure events) is not easily predictable. On the other hand, our experiments show that large failure events, even though they are only 1% of all failure events, contribute the most to unavailability. For example, the unavailability of a "pattern-aware" ERASURE$(16, 32)$ under `WS_trace` remains unchanged (0.0003) even if we remove all the small failure events. The reason is that because small failure events affect only a small number of nodes, they can be almost completely masked by data redundancy and regeneration. This explains why on the one hand, failure patterns are largely predictable, while on the other hand, pattern-aware fragment placement is not effective in improving availability. It is also worth pointing out that the sizes of these large failures still span a wide range (e.g., from 15 to over 50 in `PL_trace` and `WS_trace`). So capturing the distribution over all failure sizes is still important in the bi-exponential model.

The Design Principle. *Large correlated failures (which comprise a small fraction of all failures) have a dominant effect on system availability, and system designs must not overlook these failures. For example, failure pattern prediction techniques that work well for the bulk of correlated failures but fail for large correlated failures are not effective in alleviating the negative effects of correlated failures.*

Can Correlated Failures be Avoided by Root Cause-based Failure Pattern Prediction? We have established above that failure pattern prediction based on failure history may not be effective. By identifying the root causes of correlated failures, however, it becomes possible to predict their patterns in some cases [22]. For example, in a heterogeneous environment, nodes running the same OS may fail together due to viruses exploiting a common vulnerability.

On the other hand, first, not all root causes result in correlated failures with predictable patterns. For example, DDoS attacks result in correlated failures patterns that are inherently unpredictable. Second, it can be challenging to identify/predict root causes for all major correlated failures based on intuition. Human intuition does not reason well about close-to-zero probabilities [16]. As a result, it can be difficult to enumerate all top root causes. For example, should power failure be considered when targeting 5 nines availability? How about a certain vulnerability in a certain software? It is always possible to miss certain root causes that lead to major failures. Finally, it can also be challenging to identify/predict root causes for all major correlated failures, because the frequency of individual root causes can be extremely low. In some cases, a root cause may only demonstrate itself once (e.g., patches are usually installed after vulnerabilities are exploited). For the above reasons, we believe that while root cause analysis will help to make correlated failures more predictable, systems may never reach a point where we can predict all major correlated failures.

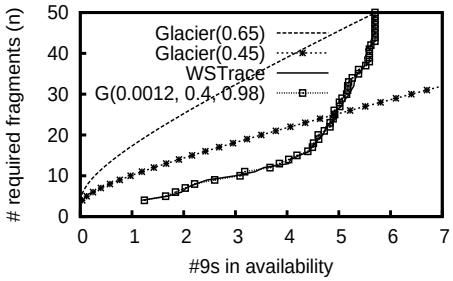

Figure 5: *Number of fragments in* ERASURE$(6, n)$ *needed to achieve certain availability targets, as estimated by Glacier's single failure size model and our distribution-based model of G(0.0012,0.4,0.98). We also plot the actual achieved availability under the trace.*

6 Is Simple Modeling of Failure Sizes Adequate?

A key challenge in system design is to obtain the "right" set of parameters that will be neither overly-pessimistic nor overly-optimistic in achieving given design goals. Because of the complexity in availability estimation introduced by failure correlation, system designers sometimes make simplifying assumptions on correlated failure sizes in order to make the problem more amenable. For example, Glacier [19] considers only the (single) maximum failure size, aiming to achieve a given availability target despite the correlated failure of up to a fraction f of all the nodes. This simplifying assumption enables the system to use a closed-form formula [19] to estimate availability and then calculate the needed m and n values in ERASURE(m, n).

Our Finding. Figure 5 quantifies the effectiveness of this approach. The figure plots the number of fragments needed to achieve given availability targets under Glacier's model (with $f = 0.65$ and $f = 0.45$) and under `WS_trace`. Glacier does not explicitly explain how f can be chosen in various systems. However, we can expect that f should

be a constant under the same deployment context (e.g., for WS_trace).

A critical point to observe in Figure 5 is that for the real trace, the curve is not a straight line (we will explore the shape of this curve later). Because the curves from Glacier's estimation are roughly straight lines, they always significantly depart from the curve under the real trace, regardless of how we tune f. For example, when $f = 0.45$, Glacier over-estimates system availability when n is large: Glacier would use ERASURE$(6, 32)$ for an availability target of 7 nines, while in fact, ERASURE$(6, 32)$ achieves only slightly above 5 nines availability. Under the same f, Glacier also under-estimates the availability of ERASURE$(6, 10)$ by roughly 2 nines. If f is chosen so conservatively (e.g., $f = 0.65$) that Glacier never over-estimates, then the under-estimation becomes even more significant. As a result, Glacier would suggest ERASURE$(6, 31)$ to achieve 3 nines availability while in reality, we only need to use ERASURE$(6, 9)$. This would unnecessarily increase the bandwidth needed to create, update, and repair the object, as well as the storage overhead, by over 240%.

While it is obvious that simplifying assumptions (such as assuming a single failure size) will always introduce inaccuracy, our above results show that the inaccuracy can be dramatic (instead of negligible) in practical settings.

The Subtlety. The reason behind the above mismatch between Glacier's estimation and the actual availability under WS_trace is that in real systems, failure sizes may cover a large range. In the limit, failure events of any size may occur; the only difference is their likelihood. System availability is determined by the combined effects of failures with different sizes. Such effects cannot be summarized as the effects of a series of failures of the same size (even with scaling factors).

To avoid the overly-pessimistic or overly-optimistic configurations resulting from Glacier's method, a system must consider a distribution of failure sizes. IRISSTORE uses the bi-exponential model for this purpose. Figure 5 also shows the number of fragments needed for a given availability target as estimated by our simulator driven by the bi-exponential model. The estimation based on our model matches the curve from WS_trace quite well. It is also important to note that the difference between Glacier's estimation and our estimation is purely from the difference between single failure size and a distribution of failure sizes. It is not because Glacier uses a formula while we use simulation. In fact, we have also performed simulations using only a single failure size, and the results are similar to those obtained using Glacier's formula.

The Design Principle. *Assuming a single failure size can result in dramatic rather than negligible inaccuracies in practice. Thus correlated failures should be modeled via a distribution.*

7 Are Additional Fragments Always Effective in Improving Availability?

Under independent failures, distributing the data always helps to improve availability, and any target availability can be achieved by using additional (smaller) fragments, without increasing the storage overhead. For this reason, system designers sometimes fix the ratio between n and m (so that the storage overhead, n/m, is fixed), and then simply increase n and m simultaneously to achieve a target availability. For instance, under independent failures, ERASURE$(16, 32)$ gives better availability than ERASURE$(12, 24)$, which, in turn, gives better availability than ERASURE$(8, 16)$. Several existing systems, including OceanStore and CFS, use such ERASURE$(n/2, n)$ schemes. Given independent failures, we can even prove that increasing the number of fragments in these schemes *exponentially* decreases unavailability:

Theorem 1 *Consider n nodes where each node fails independently with probability p and $p < 0.5$. Then there exists a constant q, $0 < q < 1$, such that $Prob$[more than $n/2$ nodes fail] $\leq q^n$ for all n.*

Proof: Directly from Hoeffding's inequality [21]. □

In Section 9, we will show that a read/write replication system using majority voting [35] for consistency has the same availability as ERASURE$(n/2, n)$. Thus, our discussion in this section also applies to these read/write replication systems (where, in this case, the storage overhead does increase with n).

Our Finding. We observe that distributing fragments across more and more machines (i.e., increasing n) may not be effective under correlated failures, even if we double or triple n. Figures 6(a) and 6(b) plot the availability of ERASURE$(4, n)$, ERASURE$(n/3, n)$ and ERASURE$(n/2, n)$ under WS_trace and PL_trace.We do not use RON_trace because it contains only 30 nodes. The three schemes clearly incur different storage overhead and achieve different availability. We do not intend to compare their availability under a given n value. Instead, we focus on the scaling trend (i.e., the availability improvement) under the three schemes when we increase n.

Both ERASURE$(n/3, n)$ and ERASURE$(n/2, n)$ suffer from a strong diminishing return effect. For example, increasing n from 20 to 60 in ERASURE$(n/2, n)$ provides less than a half nine's improvement. On the other hand, ERASURE$(4, n)$ does not suffer from such an effect. By tuning the parameters in the correlation model and using model-driven simulation, we further observe that the diminishing returns become more prominent under stronger correlation levels as well as under larger m values (see Figure 8) .

The above diminishing return shows that correlated failures prevent a system from effectively improving availabil-

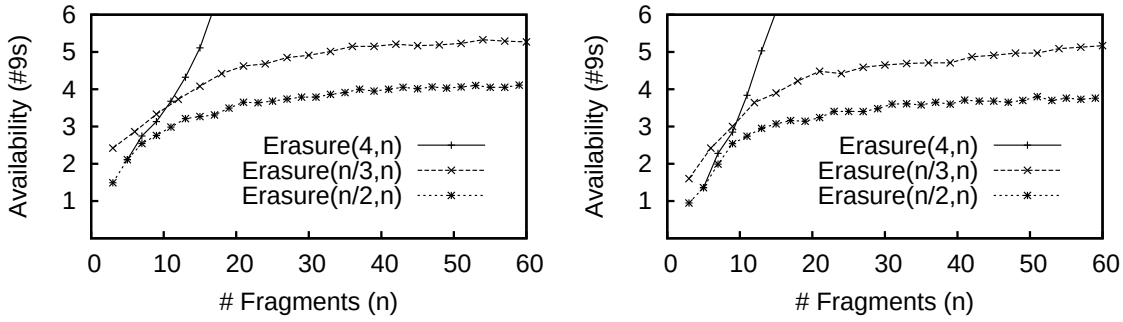

(a) ERASURE(m, n) under `WS_trace` (b) ERASURE(m, n) under `PL_trace`

Figure 6: *Availability of* ERASURE*(m, n) under different traces.*

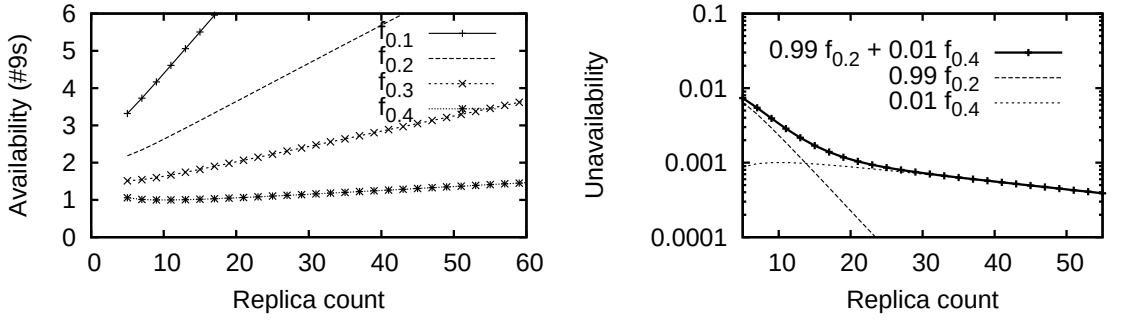

(a) ERASURE$(n/2, n)$ under one failure size (b) ERASURE$(n/2, n)$ under two failure sizes

Figure 7: *Combined effect of multiple failure sizes on the availability of* ERASURE*$(n/2, n)$. The legend f_x denotes correlated failures of x fraction of all nodes in the system, and qf_x denotes f_x happening with probability q.*

ity by distributed data across more and more machines. In read/write systems using majority voting, the problem is even worse: the same diminishing return effect occurs despite the significant increases in storage overhead.

The Subtlety. It may appear that diminishing return is an obvious consequence of failure correlation. However, somewhat surprisingly, we find that ***diminishing return does not directly result from the presence of failure correlation.***

Figure 7(a) plots the availability of ERASURE$(n/2, n)$ under synthetic correlated failures. In these experiments, the system has 277 nodes total (to match the system size in `PL_trace`), and each synthetic correlated failure crashes a random set of nodes in the system.[3] The synthetic correlated failures all have the same size. For example, to obtain the curve labeled "$f_{0.2}$", we inject correlated failure events according to Poisson arrival, and each event crashes 20% of the 277 nodes in the system. Using single-size correlated failures matches the correlation model used in Glacier's configuration analysis.

Interestingly, the curves in Figure 7(a) are roughly straight lines and exhibit no diminishing returns. If we increase the severeness (i.e., size) of the correlated failures, the only consequence is smaller slopes of the lines, instead of diminishing returns. This means that diminishing return does not directly result from correlation. Next we explain that diminishing return actually results from the combined effects of failures with different sizes (Figure 7(b)

Here we will discuss unavailability instead of availability, so that we can "sum up" unavailability values. In the real world, correlated failures are likely to have a wide range of sizes, as observed from our failure traces. Furthermore, larger failures tend to be rarer than smaller failures. As a rough approximation, system unavailability can be viewed as the summation of the unavailability caused by failures with different sizes. In Figure 7(b) failure sizes (0.2×277 and 0.4×277), where the failures with the larger size occur with smaller probability. It is interesting to see that when we add up the unavailability caused by the two

[3] Crashing *random* sets of nodes is our explicit choice for the experimental setup. The reason is exactly the same as in our bi-exponential failure correlation model (see Section 4).

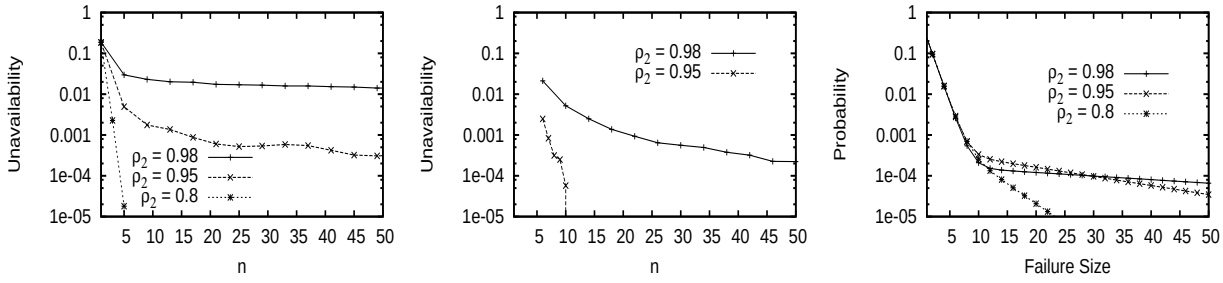

(a) ERASURE$(n/2, n)$ (b) ERASURE$(3, n)$ (c) Failure size distribution

Figure 8: *Model-driven simulation under $G(0.009, 0.4, \rho_2)$. Diminishing return becomes stronger as correlation level (ρ_2) increases or a larger m is used. In (b), when $\rho_2 = 0.8$, the unavailability is always below 10^{-5}.*

kinds of failures, the resulting curve is not a straight line.[4] In fact, if we consider nines of availability (which flips the curve over), the combined curve shows exactly the diminishing return effect.

Given the above insight, we believe that diminishing returns are likely to generalize beyond our three traces. As long as failures have different sizes and as long as larger failures are rarer than smaller failures, there will likely be diminishing returns. The only way to lessen diminishing returns is to use a smaller m in ERASURE(m, n) systems. This will make the slope of the line for $0.01 f_{0.4}$ in Figure 7(b) negative, effectively making the combined curve straighter.

The Design Principle. *System designers should be aware that correlated failures result in strong diminishing return effects in* ERASURE*(m, n) systems unless m is kept small. For popular systems such as* ERASURE*$(n/2, n)$, even doubling or tripling n provides very limited benefits after a certain point.*

8 Do Superior Designs under Independent Failures Remain Superior under Correlated Failures?

Traditionally, system designs are evaluated and compared under the assumption of independent failures. A positive answer to this question would provide support for this approach.

Our Finding. We find that correlated failures hurt some designs much more than others. Such non-equal effects are demonstrated via the example in Figure 9. Here, we plot the unavailability of ERASURE$(1, 4)$ and ERASURE$(8, 16)$ under different failure correlation levels, by tuning the parameters in our correlation model in model-driven simulation. These experiments use the model $G(0.0012, \frac{2}{5}\rho_2, \rho_2)$ (a generalization of the model for `WS_trace` to cover a range of ρ_2), and a universe of 130 nodes, with MTTF = 10 days and MTTR = 1 day. ERASURE$(1, 4)$ achieves around 1.5 fewer nines than ERASURE$(8, 16)$ when failures are independent (i.e., $\rho_2 = 0$). On the other hand, under the correlation level found in `WS_trace` ($\rho_2 = 0.98$), ERASURE$(1, 4)$ achieves 2 more nines of availability than ERASURE$(8, 16)$.[5]

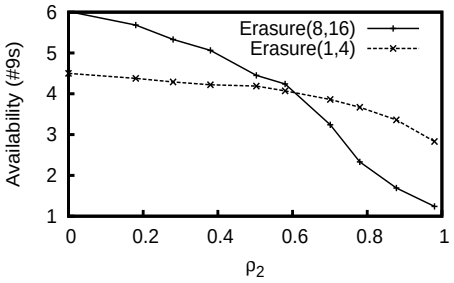

Figure 9: *Effects of the correlation model $G(0.0012, \frac{2}{5}\rho_2, \rho_2)$ on two systems. $\rho_2 = 0$ indicates independent failures, while $\rho_2 = 0.98$ indicates roughly the correlation level observed in* `WS_trace`.

The Subtlety. The cause of this (perhaps counter-intuitive) result is the diminishing return effect described earlier. As the correlation level increases, ERASURE$(8, 16)$, with its larger m, suffers from the diminishing return effect to a much greater degree than ERASURE$(1, 4)$. In general, because diminishing return effects are stronger for systems with larger m, correlated failures hurt systems with large m more than those with small m.

The Design Principle. *A superior design under independent failures may not be superior under correlated failures. In particular, correlation hurts systems with larger m more than those with smaller m. Thus designs should be explicitly evaluated and compared under correlated failures.*

[4] Note that the y-axis is on log-scale, and that is why the summation of two straight lines does not result in a third straight line.

[5] The same conclusion also holds if we directly use `WS_trace` to drive the simulation.

9 Read/Write Systems

Thus far, our discussion has focused on read-only ERASURE(m, n) systems. Interestingly, our results extend quite naturally to read/write systems that use quorum techniques or voting techniques to maintain data consistency.

Quorum systems (or voting systems) [7, 35] are standard techniques for maintaining consistency for read/write data. We first focus on the case of pure replication. Here, a user reading or writing a data object needs to access a *quorum* of replicas. For example, the majority quorum system (or majority voting) [35] requires that the user accesses a majority of the replicas. This ensures that any reader intersects in at least one replica with the latest writer, so that the reader sees the latest update. If a majority of the replicas is not available, then the data object is unavailable to the user. From an availability perspective, this is exactly the same as a read-only ERASURE$(n/2, n)$ system. Among all quorum systems that always guarantee consistency, we will consider only majority voting because its availability is provably optimal [7].

Recently, Yu [41] proposed *signed quorum systems* (SQS), which uses quorum sizes smaller than $n/2$, at the cost of a tunably small probability of reading stale data. Smaller quorum sizes help to improve system availability because fewer replicas need to be available for a data object to be available. If we do not consider regeneration (i.e, creating new replicas to compensate for lost replicas), then the availability of such SQS-based systems would be exactly the same as that of a read-only ERASURE(m, n) system, where m is the quorum size.

Regeneration makes the problem slightly more complex. It is quite tricky to ensure data consistency during regeneration in a read/write system. In IRISSTORE, we adopt previous regeneration designs from RAMBO [26], and use the Paxos distributed consensus protocol [24] to ensure consistency during regeneration. Paxos needs $n/2$ out of the n nodes to be available in order to terminate.[6] Thus, the read/write regeneration SQS-based system with a quorum size of m requires $n/2$ (instead of m) replicas to regenerate, even though only m replicas are needed for normal reads and writes. In comparison, a read-only ERASURE(m, n) system requires m fragments to regenerate, as well as m fragments for user accesses. We have performed extensive simulation of these SQS-based regeneration systems and found that our previous design principles still apply.

Finally, quorum systems can also be used over erasure-coded data [18]. Despite the complexity of these protocols, they all have simple threshold-based requirements on the number of available fragments. As a result, their availability can also be readily captured by properly adjusting the m in our ERASURE(m, n) results.

[6] It is possible to use a completely different set (and a much larger number) of nodes for Paxos to maximize its success probability [39]. Such a design will make the results for ERASURE(m, n) directly apply to a read/write replication system with a quorum size of m. Namely, the extra adjustment as described in this section is no longer needed.

10 IRISSTORE: A Highly-Available Read/Write Storage Layer

Applying the design principles in the previous sections, we have built IRISSTORE, a decentralized read/write storage layer that is highly-available despite correlated failures. IRISSTORE does not try to avoid correlated failures by predicting correlation patterns. Rather, it tolerates them by choosing the right set of parameters. IRISSTORE determines system parameters using a model with a failure size distribution rather than a single failure size. Finally, IRISSTORE explicitly quantifies and compares configurations via online simulation using our correlation model. IRISSTORE allows both replication and erasure coding for data redundancy, and also implements both majority quorum systems and SQS for data consistency. The original design of SQS [41] appropriately bounds the probability of inconsistency (e.g., probability of stale reads) when nodes MTTF and MTTR are relatively large compared to the inter-arrival time between writes and reads. If MTTF and MTTR are small compared to the write/read inter-arrival time, the inconsistency may be amplified [5]. To avoid such undesirable amplification, IRISSTORE also incorporates a simple *data refresh* technique [29].

We use IRISSTORE as the read-write storage layer of IRISLOG[7], a wide-area network monitoring system deployed on over 450+ PlanetLab nodes. IRISLOG with IRISSTORE has been available for public use for over 8 months.

At a high level, IRISSTORE consists of two major components. The first component replicates or encodes objects, and processes user accesses. The second component is responsible for regeneration, and automatically creates new fragments when existing ones fail. These two subsystems have designs similar to Om [42]. For lack of space, we omit the details (see [27]) and focus on two aspects that are unique to IRISSTORE.

10.1 Achieving Target Availability

Applications configure IRISSTORE by specifying an *availability target*, a *bi-exponential failure correlation model*, as well as a *cost function*. The correlation model can be specified by saying that the deployment context is "PlanetLab-like," "WebServer-like," or "RON-like." In these cases, IRISSTORE will use one of the three built-in failure correlation models from Section 4. We also intend to add more built-in failure correlation models in the future. To provide more flexibility, IRISSTORE also allows the application to directly specify the three tunable parameters in

[7] `http://www.intel-iris.net/irislog`

the bi-exponential distribution. It is our long term goal to extend IRISSTORE to monitor failures in the deployment, and automatically adjust the correlation model if the initial specification is not accurate.

The cost function is an application-defined function that specifies the overall cost resulting from performance overhead and inconsistency (for read/write data). The function takes three inputs, m, n, and i (for inconsistency), and returns a cost value that the system intends to minimize given that the availability target is satisfied. For example, a cost function may bound the storage overhead (i.e., n/m) by returning a high cost if n/m exceeds certain threshold. Similarly, the application can use the cost function to ensure that not too many nodes need to be contacted to retrieve the data (i.e., bounding m). We choose to leave the cost function to be completely application-specific because the requirements from different applications can be dramatically different.

With the cost function and the correlation model, IRISSTORE uses online simulation to determine the best values for m, n, and quorum sizes. It does so by exhaustively searching the parameter space (with some practical caps on n and m), and picking the configuration that minimizes the cost function while still achieving the availability target. The amount of inconsistency (i) is predicted [40, 41] based on the quorum size. Finally, this best configuration is used to instantiate the system. Our simulator takes around 7 seconds for each configuration (i.e., each pair of m and n values) on a single 2.6GHz Pentium 4; thus IRISSTORE can perform a brute-force exhaustive search for 20,000 configurations (i.e., a cap of 200 for both n and m, and $m \leq n$) in about one and a half days. Many optimizations are possible to further prune the search space. For example, if ERASURE$(16, 32)$ does not reach the availability target then neither does ERASURE$(17, 32)$. This exhaustive search is performed offline; its overhead does not affect system performance.

10.2 Optimizations for Regeneration

When regenerating read/write data, IRISSTORE (like RAMBO [26] and Om [42]) uses the Paxos distributed consensus protocol [24] to ensure consistency. Using such consistent regeneration techniques in the wide-area, however, poses two practical challenges that are not addressed by RAMBO and Om:[8]

Flooding problem. After a large correlated failure, one instance of the Paxos protocol needs to be executed for each of the objects that have lost any fragments. For example, our IRISLOG deployment on the PlanetLab has 3530 objects storing PlanetLab sensor data, and each object has 7 replicas. A failure of 42 out of 206 PlanetLab nodes (on 3/28/2004) would flood the system with 2,478 instances of Paxos. Due to the message complexity of Paxos, this creates excessive overhead and stalls the entire system.

[8] RAMBO has never been deployed over the wide-area, while Om has never been evaluated under a large number of simultaneous node failures.

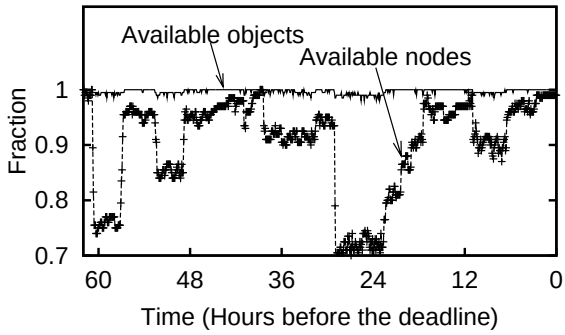

Figure 10: *Availability of* IRISSTORE *in the wild.*

Positive feedback problem. Determining whether a distant node has failed is often error-prone due to unpredictable communication delays and losses. Regeneration activity after a correlated failure increases the inaccuracy of failure detection due to the increased load placed on the network and nodes. Unfortunately, inaccurate failure detections trigger more regeneration which, in turn, results in larger inaccuracy. Our experience shows that this positive feedback loop can easily crash the entire system.

To address the above two problems, IRISSTORE implements two optimizations:

Opportunistic Paxos-merging. In IRISSTORE, if the system needs to invoke Paxos for multiple objects whose fragments *happen* to reside on the same set of nodes, the regeneration module merges all these Paxos invocations into a single one. This approach is particularly effective with IRISSTORE's load balancing algorithm [28], which tends to place the fragments for two objects either on the same set of nodes or on completely disjoint sets of nodes. Compared to explicitly aggregating objects into clusters, this approach avoids the need to maintain consistent split and merge operations on clusters.

Paxos admission-control. To avoid the positive feedback problem, we use a simple admission control mechanism on each node to control its CPU and network overhead, and to avoid excessive false failure detections. Specifically, each node, before initiating a Paxos instance, samples (by piggybacking on the periodic ping messages) the number of ongoing Paxos instances on the relevant nodes. Paxos is initiated only if the average and the maximum number of ongoing Paxos instances are below some thresholds (2 and 5, respectively, in our current deployment). Otherwise, the node queues the Paxos instance and backs off for some random time before trying again. Immediately before a queued Paxos is started, IRISSTORE rechecks whether the regeneration is still necessary (i.e., whether the object is still missing a fragment). This further improves failure

detection accuracy, and also avoids regeneration when the failed nodes have already recovered.

10.3 Availability of IRISSTORE in the Wild

In this section and the next, we report our availability and performance experience with IRISSTORE (as part of IRISLOG) on the PlanetLab over an 8-month period. IRISLOG uses IRISSTORE to maintain 3530 objects for different sensor data collected from PlanetLab nodes. As a background testing and logging mechanism, we continuously issued one query to IRISLOG every five minutes. Each query tries to access all the objects stored in IRISSTORE. We set a target availability of 99.9% for our deployment, and IRISSTORE chooses, accordingly, a replica count of 7 and a quorum size of 2.

Figure 10 plots the behavior of our deployment under stress over a 62-hour period, 2 days before the SOSP'05 deadline (i.e., 03/23/2005). The PlanetLab tends to suffer the most failures and instabilities right before major conference deadlines. The figure shows both the fraction of available nodes in the PlanetLab and the fraction of available (i.e., with accessible quorums) objects in IRISSTORE.

At the beginning of the period, IRISSTORE was running on around 200 PlanetLab nodes. Then, the PlanetLab experienced a number of large correlated failures, which correspond to the sharp drops in the "available nodes" curve (the lower curve). On the other hand, the fluctuation of the "available objects" curve (the upper curve) is consistently small, and is always above 98% even during such an unusual stress period. This means that our real world IRISSTORE deployment tolerated these large correlated failures well. In fact, the overall availability achieved by IRISSTORE during the 8-month deployment was 99.927%, demonstrating the ability of IRISSTORE to achieve a preconfigured target availability.

10.4 Basic Performance of IRISSTORE

Access latency. Figure 11(a) shows the measured latency from our lab to access a single object in our IRISLOG deployment. The object is replicated on random PlanetLab nodes. We study two different scenarios based on whether the replicas are within the US or all over the world. Network latency contributes to most of the end-to-end latency, and also to the large standard deviations.

Bandwidth usage. Our next experiment studies the amount of bandwidth consumed by regeneration, including the Paxos protocol. To do this, we consider the PlanetLab failure event on 3/28/2004 that caused 42 out of the 206 live nodes to crash in a short period of time (an event found by analyzing `PL_trace`). We replay this event by deploying IRISLOG on 206 PlanetLab nodes and then killing the IRISLOG process on 42 nodes.

Figure 11(b) plots the bandwidth used during regeneration. The failures are injected at time 100. We observe that on average, each node only consumes about 3KB/sec bandwidth, out of which 2.8KB/sec is used to perform necessary regeneration, 0.27KB/sec for unnecessary regeneration (caused by false failure detection), and 0.0083KB/sec for failure detection (pinging). The worst-case peak for an individual node is roughly 100KB/sec, which is sustainable even with home DSL links.

Regeneration time. Finally, we study the amount of time needed for regeneration, demonstrating the importance of our Paxos-merging and Paxos admission-control optimizations. We consider the same failure event (i.e., killing 42 out of 206 nodes) as above.

Figure 11(c) plots the average number of replicas per object and shows how IRISSTORE gradually regenerates failed replicas after the failure at time 100. In particular, the failure affects 2478 objects. Without Paxos admission-control or Paxos-merging, the regeneration process does not converge.

Paxos-merging reduces the total number of Paxos invocations from 2478 to 233, while admission-control helps the regeneration process to converge. Note that the average number of replicas does not reach 7 even at the end of the experiment because some objects lose a majority of replicas and cannot regenerate. A single regeneration takes 21.6sec on average which is dominated by the time for data transfer (14.3sec) and Paxos (7.3sec). The time for data transfer is determined by the amount of data and can be much larger. The convergence time of around 12 minutes is largely determined by the admission-control parameters and may be tuned to be faster. However, regeneration is typically not a time-sensitive task, because IRISSTORE only needs to finish regeneration before the next failure hits. Our simulation study based on `PL_trace` shows that 12-minute regeneration time achieves almost identical availability as, say, 5-minute regeneration time. Thus we believe IRISSTORE's regeneration mechanism is adequately efficient.

11 Simulator Validation

Sections 5-7 mainly presented simulation results for system availability. This section uses the prototype deployment of IRISSTORE to validate the accuracy of our event-driven simulator. The purpose of such validation is to confirm whether aspects that are not captured in our simulator (such as false failure detection and the Paxos queuing effects resulting from Paxos admission control) will affect the accuracy of our results. We used simulation in the paper for two reasons. First, the speed of our simulator allows us to evaluate system behavior over much longer periods. Second, simulation allows us to directly compare different system configurations by subjecting them to identical streams

Replica Location	Average Latency (ms)			Std. Dev.
	Network	Processing	Total	(ms)
USA	60	22	82	68
WORLD	165	25	190	238

(Averages and Std. Deviations are computed from 50 independent data accesses)

(a) End-to-end latency

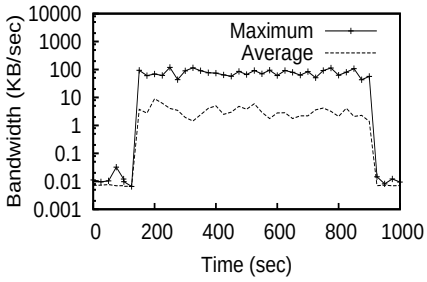

(b) Bandwidth consumption

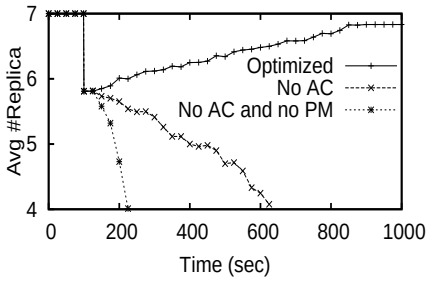

(c) Avg. # of replicas per object

Figure 11: IRISSTORE *performance. (In (c), "AC" means Paxos admission-control and "PM" means Paxos-merging.)*

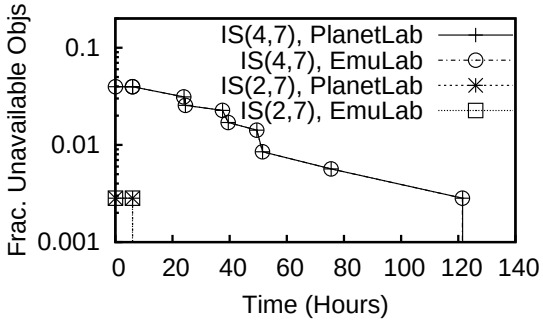

(a) PlanetLab vs. EmuLab

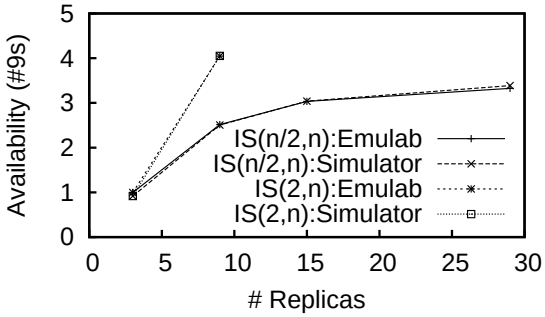

(b) Emulab vs. Simulation

Figure 12: *Validation among three testing environments.* `IS(m,n)` *means* IRISSTORE *with the configuration where each object has* n *replicas and the quorum size is* m*.*

of failure/recovery events. Unfortunately, our PlanetLab deployment must often contend with actual failures, preventing us from performing such repeatable experiments.

Our validation is performed across three testbeds: PlanetLab deployment, Emulab emulation, and event-driven simulation. Both the PlanetLab and the Emulab deployments run the real IRISSTORE code. Unlike PlanetLab, the Emulab nodes communicate over a LAN, which provides much lower latency and higher bandwidth. We use PlanetLab deployment to validate the accuracy of Emulab emulation, and then use Emulab emulation to validate event-driven simulation. We use Emulab as a bridge because we can replay longer traces on Emulab than on PlanetLab, which makes the validation results for the simulator even more convincing. We have also directly validated the simulator using PlanetLab results.

Our validation relies on replaying the same failure trace over a pair of testing environments and comparing the measured availability. When replaying traces in PlanetLab or Emulab, we speed them up by compressing the timescale of the trace so we can replay a longer trace. Specifically, for two events that are t time apart such that $t > t'$, where t' is the time needed for the system to stabilize, we replay the events time t' apart.

To validate Emulab experiments, we replay the same 7-day-long portion of `PL_trace` on PlanetLab and Emulab. This validation is performed using two different configurations: 7 replicas with quorum size of 4, and 7 replicas with quorum size of 2. Figure 12(a) plots the fraction of unavailable objects as measured in the two testbeds. Notice that the two curves from the Emulab emulation almost exactly match the two curves from the PlanetLab deployment. These results are not surprising since as shown in the previous section, each node on average consumes only 3KB/sec bandwidth, and network latency is orders of magnitude lower than regeneration time. As a result, network bandwidth and latency do not tend to significantly impact system availability.

Next, to validate our simulation results, we replay the same 30-day-long portion of `PL_trace` on Emulab and in our simulator. Figure 12(b) plots the unavailability observed from Emulab experiments and from simulation. As we can see, the results from simulation matches the emulation results nicely. These results are also expected since in our context, availability is minimally impacted by factors such as machine speed, latency, and bandwidth.

In summary, these comparisons show that the results of our event-driven simulator match closely with real system behavior. Thus, our previous findings are not artifacts of simulation and are fundamental to correlated failures.

12 Conclusion

Despite the wide awareness of correlated failures in the research community, the properties of such failures and their impact on system behavior has been poorly understood. In this paper, we made some critical steps toward helping system developers understand the impact of realistic, correlated failures on their systems. In addition, we provided a set of design principles that systems should use to tolerate such failures, and showed that some existing approaches are less effective than one might expect. We presented the design and implementation of a distributed read/write storage layer, IRISSTORE, that uses these design principles to meet availability targets even under real-world correlated failures.

Acknowledgments. We thank the anonymous reviewers and our shepherd John Byers for many helpful comments on the paper. We also thank David Anderson for giving us access to `RON_trace`, Jay Lorch for his comments on an earlier draft of the paper, Jeremy Stribling for explaining several aspects of `PL_trace`, Hakim Weatherspoon for providing the code for failure pattern prediction, Jay Wylie for providing `WS_trace`, and Praveen Yalagandula for helping us to process `PL_trace`. This research was supported in part by NSF Grant No. CNS-0435382 and funding from Intel Research.

References

[1] Akamai Knocked Out, Major Websites Offline. `http://techdirt.com/articles/20040524/0923243.shtml`.

[2] Emulab - network emulation testbed home. `http://www.emulab.net`.

[3] PlanetLab - All Pair Pings. `http://www.pdos.lcs.mit.edu/~strib/pl_app/`.

[4] The MIT RON trace. David G. Andersen, Private communication.

[5] AIYER, A., ALVISI, L., AND BAZZI, R. On the Availability of Non-strict Quorum Systems. In *DISC* (2005).

[6] BAKKALOGLU, M., WYLIE, J., WANG, C., AND GANGER, G. On Correlated Failures in Survivable Storage Systems. Tech. Rep. CMU-CS-02-129, Carnegie Mellon University, 2002.

[7] BARBARA, D., AND GARCIA-MOLINA, H. The Reliability of Voting Mechanisms. *IEEE Transactions on Computers 36*, 10 (1987).

[8] BHAGWAN, R., TATI, K., CHENG, Y., SAVAGE, S., AND VOELKER, G. M. TotalRecall: Systems Support for Automated Availability Management. In *USENIX NSDI* (2004).

[9] BOLOSKY, W. J., DOUCEUR, J. R., ELY, D., AND THEIMER, M. Feasibility of a Serverless Distributed File System Deployed on an Existing Set of Desktop PCs. In *ACM SIGMETRICS* (2000).

[10] CATES, J. Robust and Efficient Data Management for a Distributed Hash Table. Masters Thesis, Massachusetts Institute of Technology, 2003.

[11] CHUN, B., AND VAHDAT, A. Workload and Failure Characterization on a Large-Scale Federated Testbed. Tech. Rep. IRB-TR-03-040, Intel Research Berkeley, 2003.

[12] CORBETT, P., ENGLISH, B., GOEL, A., GRCANAC, T., KLEIMAN, S., LEONG, J., AND SANKAR, S. Row-Diagonal Parity for Double Disk Failure Correction. In *USENIX FAST* (2004).

[13] DABEK, F., KAASHOEK, M. F., KARGER, D., MORRIS, R., AND STOICA, I. Wide-area Cooperative Storage with CFS. In *ACM SOSP* (2001).

[14] DABEK, F., LI, J., SIT, E., ROBERTSON, J., KAASHOEK, M. F., AND MORRIS, R. Designing a DHT for Low Latency and High Throughput. In *USENIX NSDI* (2004).

[15] DOUCEUR, J. R., AND WATTENHOFER, R. P. Competitive Hill-Climbing Strategies for Replica Placement in a Distributed File System. In *DISC* (2001).

[16] FRIED, B. H. Ex Ante/Ex Post. *Journal of Contemporary Legal Issues 13*, 1 (2003).

[17] GIBBONS, P. B., KARP, B., KE, Y., NATH, S., AND SESHAN, S. IrisNet: An Architecture for a Worldwide Sensor Web. *IEEE Pervasive Computing 2*, 4 (2003).

[18] GOODSON, G., WYLIE, J., GANGER, G., AND REITER, M. Efficient Byzantine-tolerant Erasure-coded Storage. In *IEEE DSN* (2004).

[19] HAEBERLEN, A., MISLOVE, A., AND DRUSCHEL, P. Glacier: Highly Durable, Decentralized Storage Despite Massive Correlated Failures. In *USENIX NSDI* (2005).

[20] HARCHOL-BALTER, M., AND DOWNEY, A. B. Exploiting Process Lifetime Distributions for Dynamic Load Balancing. *ACM Transactions on Computer Systems 15*, 3 (1997).

[21] HOEFFDING, W. Probability Inequalities for Sums of Bounded Random Variables. *Journal of the American Statistical Association 58*, 301 (March 1963), 13–30.

[22] JUNQUEIRA, F., BHAGWAN, R., HEVIA, A., MARZULLO, K., AND VOELKER, G. Surviving Internet Catastrophes. In *USENIX Annual Technical Conference* (2005).

[23] KUBIATOWICZ, J., BINDEL, D., CHEN, Y., CZERWINSKI, S., EATON, P., GEELS, D., GUMMADI, R., RHEA, S., WEATHERSPOON, H., WEIMER, W., WELLS, C., AND ZHAO, B. OceanStore: An Architecture for Global-Scale Persistent Storage. In *ACM ASPLOS* (2000).

[24] LAMPORT, L. The Part-Time Parliament. *ACM Transactions on Computer Systems 16*, 2 (1998).

[25] LELAND, W. E., TAQQ, M. S., WILLINGER, W., AND WILSON, D. V. On the Self-similar Nature of Ethernet Traffic. In *ACM SIGCOMM* (1993).

[26] LYNCH, N., AND SHVARTSMAN, A. RAMBO: A Reconfigurable Atomic Memory Service for Dynamic Networks. In *DISC* (2002).

[27] NATH, S. *Exploiting Redundancy for Robust Sensing*. PhD thesis, Carnegie Mellon University, 2005. Tech. Rep. CMU-CS-05-166.

[28] NATH, S., GIBBONS, P. B., AND SESHAN, S. Adaptive Data Placement for Wide-Area Sensing Services. In *USENIX FAST* (2005).

[29] NATH, S., YU, H., GIBBONS, P. B., AND SESHAN, S. Tolerating Correlated Failures in Wide-Area Monitoring Services. Tech. Rep. IRP-TR-04-09, Intel Research Pittsburgh, 2004.

[30] NURMI, D., BREVIK, J., AND WOLSKI, R. Modeling Machine Availability in Enterprise and Wide-area Distributed Computing Environments. In *Euro-Par* (2005).

[31] PLANK, J. A Tutorial on Reed-Solomon Coding for Fault-Tolerance in RAID-like Systems. *Software – Practice & Experience 27*, 9 (1997).

[32] ROWSTRON, A., AND DRUSCHEL, P. Storage Management and Caching in PAST, A Large-scale, Persistent Peer-to-peer Storage Utility. In *ACM SOSP* (2001).

[33] SHI, J., AND MALIK, J. Normalized Cuts and Image Segmentation. *IEEE Transactions on Pattern Analysis and Machine Intelligence 22*, 8 (2000).

[34] TANG, D., AND IYER, R. K. Analysis and Modeling of Correlated Failures in Multicomputer Systems. *IEEE Transactions on Computers 41*, 5 (1992).

[35] THOMAS, R. H. A Majority Consensus Approach to Concurrency Control for Multiple Copy Databases. *ACM Transactions on Database Systems 4*, 2 (1979).

[36] WEATHERSPOON, H., CHUN, B.-G., SO, C. W., AND KUBIATOWICZ, J. Long-Term Data Maintenance: A Quantitative Approach. Tech. Rep. UCB/CSD-05-1404, University of California, Berkeley, 2005.

[37] WEATHERSPOON, H., MOSCOVITZ, T., AND KUBIATOWICZ, J. Introspective Failure Analysis: Avoiding Correlated Failures in Peer-to-Peer Systems. In *IEEE RPPDS* (2002).

[38] YALAGANDULA, P., NATH, S., YU, H., GIBBONS, P. B., AND SESHAN, S. Beyond Availability: Towards a Deeper Understanding of Machine Failure Characteristics in Large Distributed Systems. In *USENIX WORLDS* (2004).

[39] YIN, J., MARTIN, J., VENKATARAMANI, A., ALVISI, L., AND DAHLIN, M. Separating Agreement from Execution for Byzantine Fault Tolerant Services. In *ACM SOSP* (2003).

[40] YU, H. Overcoming the Majority Barrier in Large-Scale Systems. In *DISC* (2003).

[41] YU, H. Signed Quorum Systems. In *ACM PODC* (2004).

[42] YU, H., AND VAHDAT, A. Consistent and Automatic Replica Regeneration. *ACM Transactions on Storage 1*, 1 (2005).